JACS
JOURNAL OF THE AMERICAN CHEMICAL SOCIETY
Communication
pubs.acs.org/JACS

Metalation Triggers Single Crystalline Order in a Porous Solid

Yun-Long Hou,[†,⊥] Ka-Kit Yee,[†,⊥] Yan-Lung Wong,[†,⊥] Meiqin Zha,[†] Jun He,[#] Matthias Zeller,[‡] Allen D. Hunter,[§] Kaiqi Yang,[†] and Zhengtao Xu*[,†]

[†]Department of Biology and Chemistry, City University of Hong Kong, 83 Tat Chee Avenue, Kowloon, Hong Kong, China
[#]School of Chemical Engineering and Light Industry, Guangdong University of Technology, Guangzhou 510006, Guangdong, China
[‡]Department of Chemistry, Purdue University, 610 Purdue Mall, West Lafayette, Indiana 47907, United States
[§]Department of Chemistry, Youngstown State University, One University Plaza, Youngstown, Ohio 44555, United States

Supporting Information

ABSTRACT: We report the dramatic triggering of structural order in a Zr(IV)-based metal−organic framework (MOF) through docking of $HgCl_2$ guests. Although as-made crystals were unsuitable for single crystal X-ray diffraction (SCXRD), with diffraction limited to low angles well below atomic resolution due to intrinsic structural disorder, permeation of $HgCl_2$ not only leaves the crystals intact but also resulted in fully resolved backbone as well as thioether side groups. The crystal structure revealed elaborate $HgCl_2$-thioether aggregates nested within the host octahedra to form a hierarchical, multifunctional net. The chelating thioether groups also promote Hg(II) removal from water, while the trapped Hg(II) can be easily extricated by 2-mercaptoethanol to reactivate the MOF sorbent.

Single crystal X-ray diffraction (SCXRD) remains all-important for characterizing porous materials because of its ability to reveal precisely the atomistic array. Organic-based systems with increasingly larger pores and complex functionalities (such as metal−organic frameworks and polyhedra[1]), however, often present grave challenges for SCXRD studies. One fundamental issue arises from the dynamic and flexible nature of these organic open structures, which often features highly aggravated atomic motion and disorder. Notably, severely disordered linkers and nodes often frustrate SCXRD analysis even for systems that form into large crystal-like monoliths. Namely, even though the average positions of the individual linkers (and the nodes) are evenly spaced to provide long-range order, i.e., the typical translational symmetry that underpins macroscopically appealing crystals, locally the linkers and nodes can still wiggle and shift to compromise severely the resolution of the atomic positions. For long flexible linkers, atoms halfway between the nodes can shift by several Ångstroms, placing them well beyond atomic resolution. Even greater difficulty exists for associated guests or flexible side chains that extend into the pore domain, as these may not only be disordered with the ill-defined parts of linkers, but they generally behave like liquids and even enhanced radiation sources do not necessarily ameliorate the situation. Efforts to locate and determine guest molecules therefore entail well-defined, significant interaction with the host grid.[2]

That is why we have been pondering postcrystallization treatments for enhancing the structural order of complex MOF solids. For this, the practice of soaking crystals in heavy metal solutions in protein crystallography is instructive. Therein, heavy atoms were introduced into the unit cell to help solve the crystal structure by overcoming the phase problem (i.e., the Patterson method). Similar metalation procedures are also applied to MOF crystals,[3] but here the main intent remains simply to introduce the metal function, while inserting metal guests to facilitate expressly SCXRD analyses remains unexplored. In cases of single-crystal-to-single-crystal transformations, metal centers inserted into MOF hosts were often not located by SCXRD, with only a few exceptions in which metal-binding sites were built into the rigid host backbone.[3b,4]

The present case thus constitutes a sharp contrast, not only because of the $HgCl_2$-induced structural order in a topical Zr(IV)-based MOF but also for the elaborate $HgCl_2$-side chain aggregate assembled at the pore region. The exercise here builds on our long-standing effort in the hard-and-soft chemistry of carboxylic linkers with sulfur functions,[5] and bears closely upon the application of mercury removal. To boost mercury uptake, we installed a pentaerythrityl side chain equipped with three-pronged thioether donors (**M1**; Figure 1). Unlike the very reactive thiol groups, which tend to bind covalently mercury and complicate absorbent recycling (e.g., involving strong HCl treatment),[6] chelating thioether units provide more tunable binding strength to allow the bound Hg species to be extricated. Here we report a porous network based on Zr(IV) and **M1**, wherein dramatic enhancement of crystalline order were triggered by the introduction of $HgCl_2$ guests. The highly ordered thioether-$HgCl_2$ domain (as determined by SCXRD) occupies the octahedral void of the host net, generating a rare cage-in-cage, and net-in-net hierarchy in the host−guest assembly.

A solvothermal reaction of **M1** (Scheme S1) and $ZrCl_4$ yielded light-yellow octahedral crystals of Zr-**M1** (Figure 1). Results of elemental and thermogravimetric (TG) analyses, and solution ^1H NMR measurement (on the dissolved sample) are consistent with the formula $Zr_6O_4(OH)_4(\mathbf{M1})_6$ associated with guest molecules of benzoic acid, DEF and water (see SI). The as-made crystals feature a powder X-ray diffraction pattern

Received: September 18, 2016
Published: October 31, 2016

DOI: 10.1021/jacs.6b09763
J. Am. Chem. Soc. 2016, 138, 14852−14855

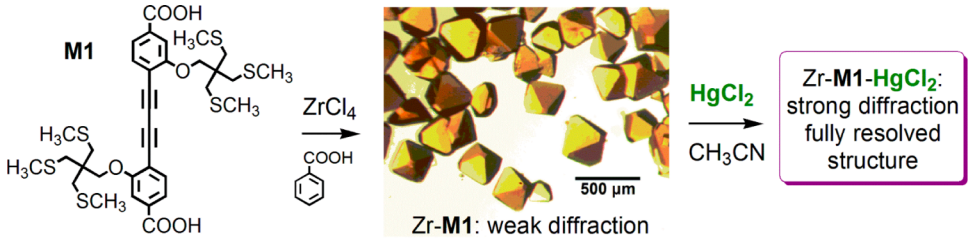

Figure 1. Synthetic scheme for the Zr-**M1** crystals (photo shown in the middle) and the $HgCl_2$ uptake to form Zr-**M1**-$HgCl_2$.

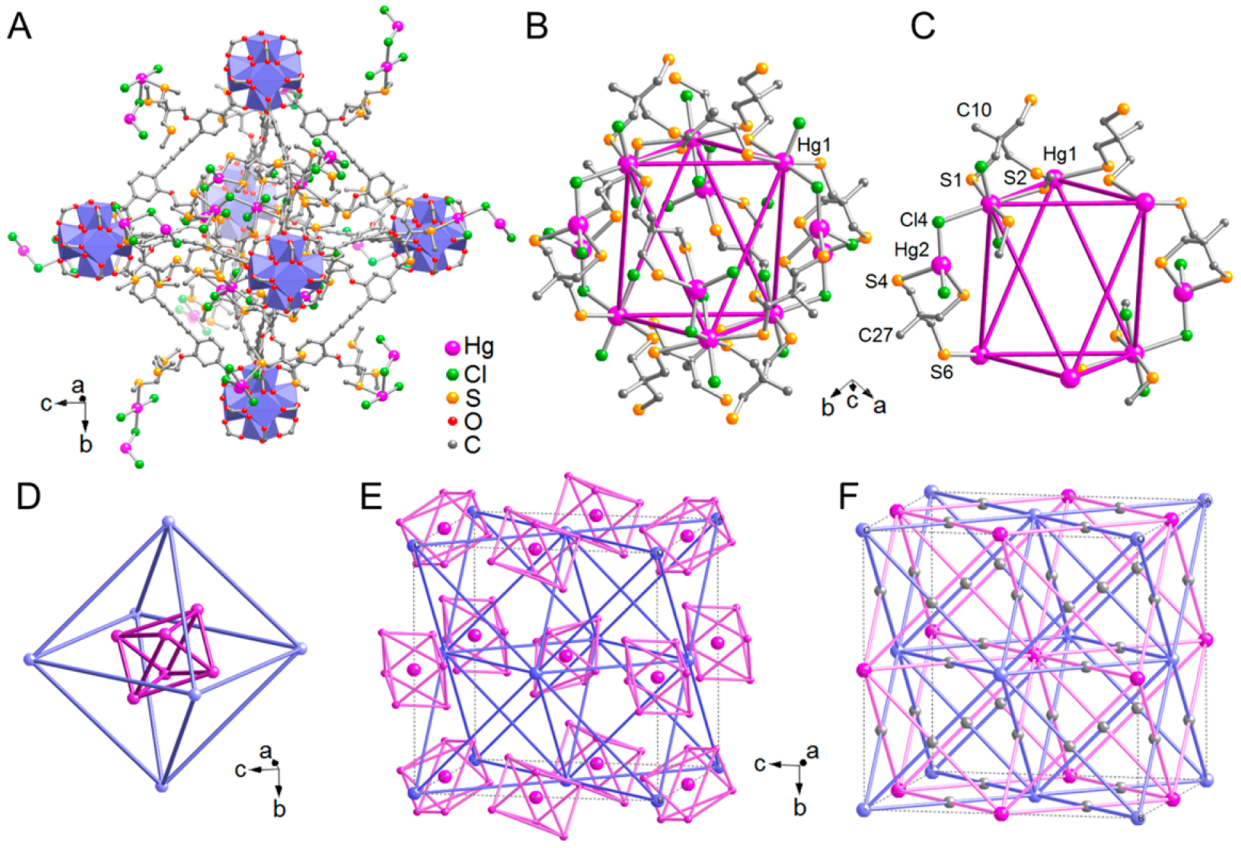

Figure 2. Single-crystal structure of Zr-**M1**-$HgCl_2$. (a) An octahedral unit based on Zr−O clusters (violet) and **M1** linkers, with the thioether side chains and Hg_2Cl_4 dimers shown. Spheres coding for Hg, Cl, S, O, C is listed to the lower right. (b) The 12 thioether side chains and six Hg_2Cl_4 units inside the octahedral cage. The six bridges (magenta; 8.360 and 10.350 Å) across the Hg1 sites outline the secondary octahedron. For clarity, the methyl ends are omitted. (c) A simplification of panel b for highlighting the chemical connectivity of the artistically rendered Hg1−Hg1 bridges. (d) A geometrical abstraction of the two nested cages: the outer one builds on the Zr−O cluster and **M1** backbones; the inner one builds on the contained thioether-$HgCl_2$ aggregate, and is simplified using the Hg1 as apexes. (e) A unit cell based on the abstraction of panel d, showing violet spheres (i.e., Zr−O cluster) at the corners and face centers, and magenta spheres (i.e., center of the inner cage) halfway on the edges. (f) A topological representation of panel e: the **M1** linker (abstracted as a small gray sphere) is 4-connected, with two violet connections (i.e., to the Zr−O cluster) crossed by two magenta ones (i.e., to the thioether-Hg cages).

indicative of the UiO prototype (Figure S4, patterns a and b), which consists of an fcc (face-centered cubic) array of $Zr_6O_4(OH)_4$ clusters bridged by the linear linkers. However, attempts to obtain a single crystal structure were thwarted because only weak diffraction spots at low angles were observed (Figure S5), indicating highly disordered and diffuse atomic positions in the as-made crystals of Zr-**M1**.

Dramatic improvement of the X-ray data set, however, was achieved when the Zr-**M1** crystals were immersed in an acetonitrile solution of $HgCl_2$. The resultant $HgCl_2$-loaded sample (Zr-**M1**-$HgCl_2$) was solved in the cubic space group $Pn\bar{3}$ (No. 201). Unlike the disorder and diffuse features of side chains often observed in open structures, the thioether side chains, the backbones as well as the encapsulated $HgCl_2$ guests in Zr-**M1**-$HgCl_2$ were all distinctly resolved from the X-ray diffraction data set (Figures 2 and 3), with only minor static disorder limited to some side chain atoms (see SI). The host net features the UiO topology, with the side chains and the $HgCl_2$ guests confined within the octahedral cavities, leaving the tetrahedral ones unoccupied.

The structurally resolved side chain-guest domain in the octahedral cage provides a rare glimpse into an elaborate self-assembly behavior within a porous host net. Taken together, each octahedral cage of the Zr-MOF host grid contains 12 tris(methylthiomethyl)methyl side groups bonded to 12 $HgCl_2$ sites (refined as partially occupied, see SI for details). The

DOI: 10.1021/jacs.6b09763
J. Am. Chem. Soc. 2016, 138, 14852−14855

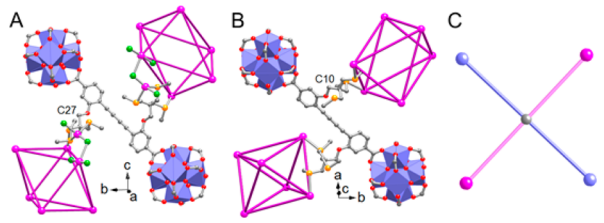

Figure 3. Local bonding of the two crystallographically independent **M1** linkers (panels a and b). Each **M1** linker connects to two Zr−O clusters (shown as violet polyhedra) via the carboxyl ends, and two $HgCl_2$-based octahedral blocks (magenta) via the thioether pendant groups. In panel a, all S atoms are coordinated to Hg(II); in panel b, only two of the three S atoms on each side group bond to Hg(II). Topologically, both **M1** linkers are 4-connected as shown in panel c. The same color code as Figure 2 is used.

structure features two crystallographically distinct sets of $HgCl_2$ units (Hg1 and Hg2) and side groups (that of C10 and that of C27; Figure 2b,c; Figure 3a,b). The C10 side groups straddles two Hg1 atoms (Hg1−S2, 3.024 Å; Hg1−S1, 3.063 Å), with the third sulfur atom being uncoordinated; all three S atoms on the C27 side group, by comparison, are coordinated, with two chelating an Hg2 atom (Hg2−S4, 2.760; Hg2−S5, 2.667 Å), and the third one bridging onto an Hg1 atom (Hg1−S6, 3.021 Å). The Hg1 and Hg2 are bridged by a chlorine atom (Cl4; Hg1−Cl4, 2.972 Å; Hg2−Cl4, 2.334 Å) to form a dimeric Hg_2Cl_4 unit. Hg1 is also bonded to two terminal Cl atoms (at shorter Hg1−Cl distances of 2.345 and 2.372 Å): together with the weaker-bonded bridging Cl4, and the three relatively distant S atoms (at 3.021−3.063 Å), Hg1 is 6-coordinated with a near-octahedral geometry. By comparison, Hg2 is tetrahedrally bonded, but features shorter distances to the S and Cl donors.

The six Hg_2Cl_4 units constitute the apexes of a distorted octahedron, while the 12 side groups follow the edges. In Figure 2b, the six Hg1 atoms were taken as the apexes to outline the octahedron, which is elongated along the $\bar{3}$ axis. As shown in Figure 2c, the top and bottom triangles involve the C10 side groups, while the C27 side groups (together with Hg2 and Cl4) constitute the longer edges a cross the two triangles. The inner cavity of the subsidiary octahedron measures about 4.7 Å, and is found to be vacant.

The hierarchy of the structure can be viewed in two perspectives. One is local, focusing on each host octahedron [i.e., with each apex occupied by a $Zr_6O_4(OH)_4$ cluster] as the primary cage, with the secondary cage being that formed by the 12 thioether side groups and the associated $HgCl_2$ moieties (Figure 2d). Compared with other cage-in-cage structures,[7] most of which were assembled all at once in one-pot synthesis, Zr-**M1**-$HgCl_2$ represents a rare single-crystalline system in which the secondary cage was constructed by guest insertion. Such a sequential and reversible installation of the secondary cage offers the advantages of flexibility, as it allows a variety of metal ions to be inserted for self-assembly within the host net.

The other perspective is global, and focuses on how dialing in the Hg subcages impacts the fcc, UIO-type host net (the Zr net). Notice the Hg subcages per se form an fcc net (the Hg net), as they occupy the body center and the edge middle of the fcc cell of the Zr net (resembling the NaCl structure; Figure 2e,f). Herein, the thioether side chains and part of the **M1** backbone (Figure 3) serve to link up the Hg subcages. The Hg subcages thus transform **M1** from a ditopic into a tetratopic linker. As it were, the Zr net and the Hg net intersect at the **M1** molecule to give rise to a 4,12-connected net of the **ftw** topology (the NU-1100 net).[8] Interestingly, this (4,12)-net formally features a smaller fcc unit wherein the eight corners are taken by the Zr nodes and Hg nodes and the face centers by the **M1** nodes. Such a subsidiary fcc unit, arising from installing the Hg subcages and accounting for 1/8 of the original fcc cell of the host Zr net, constitute a distinct structural hierarchy in the solid state.

The chelating thioether-$HgCl_2$ interactions point to effective mercury removal. To explore mercury capture from water, as-made Zr-**M1** (~10 mg) was placed in a solution of $Hg(NO_3)_2$ (8.0 ppm; 10 mL; containing 1.3% HNO_3). After being stirred at room temperature (rt) for 20 h, the residual Hg(II) was found to be lower than 0.27 ppm (by ICP-AES and diphenylthiocarbazone extraction method, see Figure S6), i.e., over 96% of the mercury was removed by Zr-**M1**. The mercury affinity was evaluated yielding a distribution coefficient K_d of 1.47×10^4 mL g^{-1}. Such a K_d value is on par with some commercially available resins, even though stronger-chelating thioether groups could likely boost the mercury binding to approach the K_d values of thiol-based systems (e.g., 10^5−10^7).[6]

The adsorption isotherm data was fitted with the Langmuir model (Figures 4) with a high correlation coefficient (R >

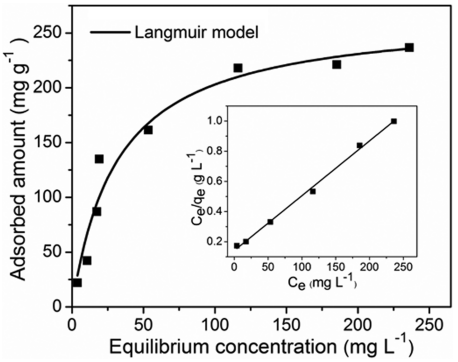

Figure 4. A Hg(II) Langmuir sorption isotherm for Zr-**M1**. Inset: linear expression fitted with the Langmuir model.

0.996). The maximum adsorption capacity of mercury ions was calculated to be 275 mg g^{-1}, which is consistent with the mercury content (Hg/Zr-**M1** = 249/1000) determined from the single crystal structure of Zr-**M1**-$HgCl_2$.

Unlike the stronger-binding thiol group, thioether groups coordinate to Hg(II) ions more reversibly, and they can be deployed in various chelating motifs to combine binding strength and ease of regeneration. Specifically, the majority (over 96%) of the $HgCl_2$ captured in Zr-**M1**-$HgCl_2$ can be extricated by simply stirring with an acetonitrile solution of 2-mercaptoethanol at rt, without strong acids or bases as often entailed in thiol-based sorbents. The structural integrity of solid adsorbent of Zr-**M1** thus recovered was confirmed by its PXRD pattern matching that of as made Zr-**M1** (Figure S4, pattern e). To illustrate recyclability, the capture-release cycle was executed four times (see SI). Although the K_d values were found to remain on the order of 10^4, the crystallinity of the Zr-**M1** remained intact as examined by PXRD (pattern f in Figure S4).

In conclusion, we have developed a thioether-tagged MOF as a recyclable sorbent for removing Hg from water. Moreover, the heavy atom insertion into the intrinsically disordered MOF solid greatly enhances the structural order to render a well-

DOI: 10.1021/jacs.6b09763
J. Am. Chem. Soc. 2016, 138, 14852−14855

defined SCXRD solution, and to produce a rare cage-in-cage and net-in-net hierarchy. We are experimenting with the docking of Ag, Pb and other heavy atoms, in order to test the generality of the crystallographic ordering process, and to enable further SCXRD to tackle the structures of ever more complex MOF solids.

■ ASSOCIATED CONTENT

Supporting Information

The Supporting Information is available free of charge on the ACS Publications website at DOI: 10.1021/jacs.6b09763.

Experimental procedure and additional data, including NMR spectra, TGA plots, PXRD patterns (PDF)
Crystallographic information (CIF)

■ AUTHOR INFORMATION

Corresponding Author

*zhengtao@cityu.edu.hk.

Author Contributions

⊥These authors contribute equally.

Notes

The authors declare no competing financial interest.

■ ACKNOWLEDGMENTS

This work is supported by the Research Grants Council of HKSAR (CityU 103407), the National Natural Science Foundation of China (21471037) and Guangdong Natural Science Funds for Distinguished Young Scholar (15ZK0307). The diffractometer at Youngstown State University was funded by NSF grant 1337296.

■ REFERENCES

(1) (a) Cook, T. R.; Zheng, Y.-R.; Stang, P. J. *Chem. Rev.* **2013**, *113*, 734−777. (b) Cook, T. R.; Stang, P. J. *Chem. Rev.* **2015**, *115*, 7001−7045. (c) Wang, C.; Liu, D.; Lin, W. *J. Am. Chem. Soc.* **2013**, *135*, 13222−13234. (d) Xu, Z. *Metal−Organic Frameworks: Semiconducting Frameworks*; John Wiley & Sons, Ltd: Chichester, 2014;. (e) Li, B.; Chrzanowski, M.; Zhang, Y.; Ma, S. *Coord. Chem. Rev.* **2016**, *307*, 106−129. (f) Zhang, M.; Gu, Z.-Y.; Bosch, M.; Perry, Z.; Zhou, H.-C. *Coord. Chem. Rev.* **2015**, *293−294*, 327−356. (g) Sun, L.; Campbell, M. G.; Dincă, M. *Angew. Chem., Int. Ed.* **2016**, *55*, 3566−3579. (h) Guillerm, V.; Kim, D.; Eubank, J. F.; Luebke, R.; Liu, X.; Adil, K.; Lah, M. S.; Eddaoudi, M. *Chem. Soc. Rev.* **2014**, *43*, 6141−6172. (i) Deria, P.; Mondloch, J. E.; Karagiaridi, O.; Bury, W.; Hupp, J. T.; Farha, O. K. *Chem. Soc. Rev.* **2014**, *43*, 5896−5912. (j) Perry, J. J. I. V.; Perman, J. A.; Zaworotko, M. J. *Chem. Soc. Rev.* **2009**, *38*, 1400−1417. (k) Tranchemontagne, D. J.; Ni, Z.; O'Keeffe, M.; Yaghi, O. M. *Angew. Chem., Int. Ed.* **2008**, *47*, 5136−5147. (l) He, J.; Zeller, M.; Hunter, A. D.; Xu, Z. *CrystEngComm* **2015**, *17*, 9254−9263.

(2) (a) Lee, S.; Kapustin, E. A.; Yaghi, O. M. *Science* **2016**, *353*, 808−811. (b) Urban, S.; Brkljaca, R.; Hoshino, M.; Lee, S.; Fujita, M. *Angew. Chem., Int. Ed.* **2016**, *55*, 2678−2682. (c) Yoshioka, S.; Inokuma, Y.; Duplan, V.; Dubey, R.; Fujita, M. *J. Am. Chem. Soc.* **2016**, *138*, 10140−10142.

(3) (a) Doonan, C. J.; Morris, W.; Furukawa, H.; Yaghi, O. M. *J. Am. Chem. Soc.* **2009**, *131*, 9492−9493. (b) Zhou, X.-P.; Xu, Z.; Zeller, M.; Hunter, A. D. *Chem. Commun.* **2009**, 5439−5441. (c) Bloch, E. D.; Britt, D.; Lee, C.; Doonan, C. J.; Uribe-Romo, F. J.; Furukawa, H.; Long, J. R.; Yaghi, O. M. *J. Am. Chem. Soc.* **2010**, *132*, 14382−14384. (d) Wu, C.-D.; Hu, A.; Zhang, L.; Lin, W. *J. Am. Chem. Soc.* **2005**, *127*, 8940−8941. (e) Yee, K.-K.; Reimer, N.; Liu, J.; Cheng, S.-Y.; Yiu, S.-M.; Weber, J.; Stock, N.; Xu, Z. *J. Am. Chem. Soc.* **2013**, *135*, 7795−7798. (f) Yee, K.-K.; Wong, Y.-L.; Zha, M.; Adhikari, R. Y.; Tuominen, M. T.; He, J.; Xu, Z. *Chem. Commun.* **2015**, *51*, 10941−10944. (g) Gui, B.; Yee, K.-K.; Wong, Y.-L.; Yiu, S.-M.; Zeller, M.; Wang, C.; Xu, Z. *Chem. Commun.* **2015**, *51*, 6917−6920. (h) Manna, K.; Zhang, T.; Greene, F. X.; Lin, W. *J. Am. Chem. Soc.* **2015**, *137*, 2665−2673. (i) Falkowski, J. M.; Sawano, T.; Zhang, T.; Tsun, G.; Chen, Y.; Lockard, J. V.; Lin, W. *J. Am. Chem. Soc.* **2014**, *136*, 5213−5216. (j) Fei, H.; Cohen, S. M. *J. Am. Chem. Soc.* **2015**, *137*, 2191−2194. (k) Chang, G.; Huang, M.; Su, Y.; Xing, H.; Su, B.; Zhang, Z.; Yang, Q.; Yang, Y.; Ren, Q.; Bao, Z.; Chen, B. *Chem. Commun.* **2015**, *51*, 2859−2862. (l) Schröder, F.; Esken, D.; Cokoja, M.; van den Berg, M. W. E.; Lebedev, O. I.; Van Tendeloo, G.; Walaszek, B.; Buntkowsky, G.; Limbach, H.-H.; Chaudret, B.; Fischer, R. A. *J. Am. Chem. Soc.* **2008**, *130*, 6119−6130. (m) Jiang, H.-L.; Liu, B.; Akita, T.; Haruta, M.; Sakurai, H.; Xu, Q. *J. Am. Chem. Soc.* **2009**, *131*, 11302−11303. (n) Evans, J. D.; Sumby, C. J.; Doonan, C. J. *Chem. Soc. Rev.* **2014**, *43*, 5933−5951. (o) Mondloch, J. E.; Bury, W.; Fairen-Jimenez, D.; Kwon, S.; DeMarco, E. J.; Weston, M. H.; Sarjeant, A. A.; Nguyen, S. T.; Stair, P. C.; Snurr, R. Q.; Farha, O. K.; Hupp, J. T. *J. Am. Chem. Soc.* **2013**, *135*, 10294−10297.

(4) (a) Gonzalez, M. I.; Bloch, E. D.; Mason, J. A.; Teat, S. J.; Long, J. R. *Inorg. Chem.* **2015**, *54*, 2995−3005. (b) Bloch, W. M.; Burgun, A.; Coghlan, C. J.; Lee, R.; Coote, M. L.; Doonan, C. J.; Sumby, C. J. *Nat. Chem.* **2014**, *6*, 906−912.

(5) (a) Zhou, X.-P.; Xu, Z.; Zeller, M.; Hunter, A. D.; Chui, S. S.-Y.; Che, C.-M. *Inorg. Chem.* **2008**, *47*, 7459−7461. (b) He, J.; Yang, C.; Xu, Z.; Zeller, M.; Hunter, A. D.; Lin, J. *J. Solid State Chem.* **2009**, *182*, 1821−1826. (c) Cui, J.; Wong, Y.-L.; Zeller, M.; Hunter, A. D.; Xu, Z. *Angew. Chem., Int. Ed.* **2014**, *53*, 14438−14442. (d) He, J.; Yee, K.-K.; Xu, Z.; Zeller, M.; Hunter, A. D.; Chui, S. S.-Y.; Che, C.-M. *Chem. Mater.* **2011**, *23*, 2940−2947.

(6) Li, B.; Zhang, Y.; Ma, D.; Shi, Z.; Ma, S. *Nat. Commun.* **2014**, *5*, 5537.

(7) (a) Zheng, S.-T.; Wu, T.; Irfanoglu, B.; Zuo, F.; Feng, P.; Bu, X. *Angew. Chem., Int. Ed.* **2011**, *50*, 8034−8037. (b) Zheng, S.-T.; Bu, J. T.; Li, Y.-F.; Wu, T.; Zuo, F.; Feng, P.-Y.; Bu, X.-H. *J. Am. Chem. Soc.* **2010**, *132*, 17062−17064. (c) Tian, D.; Chen, Q.; Li, Y.; Zhang, Y.-H.; Chang, Z.; Bu, X.-H. *Angew. Chem., Int. Ed.* **2014**, *53*, 837−841. (d) Sun, Q.-F.; Murase, T.; Sato, S.; Fujita, M. *Angew. Chem., Int. Ed.* **2011**, *50*, 10318−10321. (e) Qiu, X.; Zhong, W.; Bai, C.; Li, Y. *J. Am. Chem. Soc.* **2016**, *138*, 1138−1141.

(8) (a) Gutov, O. V.; Bury, W.; Gomez-Gualdron, D. A.; Krungleviciute, V.; Fairen-Jimenez, D.; Mondloch, J. E.; Sarjeant, A. A.; Al-Juaid, S. S.; Snurr, R. Q.; Hupp, J. T.; Yildirim, T.; Farha, O. K. *Chem. - Eur. J.* **2014**, *20*, 12389−12393. (b) Deria, P.; Gomez-Gualdron, D. A.; Bury, W.; Schaef, H. T.; Wang, T. C.; Thallapally, P. K.; Sarjeant, A. A.; Snurr, R. Q.; Hupp, J. T.; Farha, O. K. *J. Am. Chem. Soc.* **2015**, *137*, 13183−13190. (c) Morris, W.; Volosskiy, B.; Demir, S.; Gandara, F.; McGrier, P. L.; Furukawa, H.; Cascio, D.; Stoddart, J. F.; Yaghi, O. M. *Inorg. Chem.* **2012**, *51*, 6443−6445.

DOI: 10.1021/jacs.6b09763
J. Am. Chem. Soc. 2016, 138, 14852−14855